

Integrated Microfluidic Electrochemical DNA Sensor

Brian S. Ferguson,[†] Steven F. Buchsbaum,[‡] James S. Swensen,^{†,§} Kuangwen Hsieh,[†] Xinhui Lou,[†] and H. Tom Soh^{*,†,§}

Department of Mechanical Engineering, University of California, Santa Barbara, California 93106, College of Creative Studies, Physics, University of California, Santa Barbara, California 93106, and Department of Materials, University of California, Santa Barbara, California 93106

Effective systems for rapid, sequence-specific nucleic acid detection at the point of care would be valuable for a wide variety of applications, including clinical diagnostics, food safety, forensics, and environmental monitoring. Electrochemical detection offers many advantages as a basis for such platforms, including portability and ready integration with electronics. Toward this end, we report the Integrated Microfluidic Electrochemical DNA (IMED) sensor, which combines three key biochemical functionalities—symmetric PCR, enzymatic single-stranded DNA generation, and sequence-specific electrochemical detection—in a disposable, monolithic chip. Using this platform, we demonstrate detection of genomic DNA from *Salmonella enterica* serovar Typhimurium LT2 with a limit of detection of <10 aM, which is ~2 orders of magnitude lower than that from previously reported electrochemical chip-based methods.

Sequence-specific detection of very low quantities of DNA or RNA at the point of care is useful for a wide range of applications, including clinical diagnostics,¹ food safety testing,² forensics,³ and environmental monitoring.⁴ For such applications, direct detection without amplification is difficult, because the amount of nucleic acids available from samples typically falls below 20 fM (35 $\mu\text{g}/\text{mL}$),^{5,6} and there has been considerable interest in integrating nucleic acid amplification with quantitative, sequence-specific detection through the use of microfluidics technology. For example, many investigators have performed on-chip integration of polymerase chain reaction (PCR) with a variety of detection methodologies, including capillary electrophoresis,⁷ hybridization arrays,⁸ intercalating dyes,^{9,10} and Taqman probes.¹¹

Electrochemical approaches offer an attractive detection modality, because they require minimal instrumentation and are readily integrated with microelectronics in a chip-based format,¹² and several investigators have shown significant progress with such systems. For example, Liu et al. demonstrated asymmetric PCR with a two-step electrochemical hybridization sensor using ferrocene labels to achieve ~2 fM detection of bacterial DNA.^{13,14} Yeung et al. integrated asymmetric PCR with multiplexed detection at 1 fM through the use of electrode-specific probe immobilization.¹⁵ More recently, the same group demonstrated an improved means of performing quantitative electrochemical detection during PCR with a limit of detection of 5 fM.¹⁶ Because most hybridization-based detection schemes require single-stranded DNA (ssDNA) targets, asymmetric PCR has been extensively used to generate ssDNA amplicons, as illustrated by the aforementioned examples. Unfortunately, the yield of asymmetric PCR is limited by linear rather than exponential amplification, and it is thus inherently less efficient than symmetric PCR and requires significantly longer reaction times.^{17,18}

To overcome these limitations, symmetric PCR may be performed with a modified primer, followed by exonuclease-mediated digestion to generate single strands as done by Reske et al. and Luo et al.^{19,20} Here, we present the first work to integrate similar symmetric PCR, ssDNA generation, and sequence-specific electrochemical detection on a single monolithic chip toward a point-of-care system: the Integrated Microfluidic Electrochemical

* To whom correspondence should be addressed. Tel.: 1-805-893-8737. Fax: 1-805-893-8651. E-mail: tsoh@engineering.ucsb.edu.

[†] Department of Mechanical Engineering.

[‡] College of Creative Studies, Physics.

[§] Department of Materials.

- (1) Yang, S.; Rothman, R. E. *Lancet Infect. Dis.* **2004**, *4*, 337–348.
- (2) Palchetti, I.; Mascini, M. *Anal. Bioanal. Chem.* **2008**, *391*, 455–471.
- (3) Carey, L.; Mitnik, L. *Electrophoresis* **2002**, *23*, 1386–1397.
- (4) Gardeniers, J. G. E.; van den Berg, A. *Anal. Bioanal. Chem.* **2004**, *378*, 1700–1703.
- (5) Wilhelm, J.; Pingoud, A. *ChemBioChem* **2003**, *4*, 1120–1128.
- (6) Goodrich, T. T.; Lee, H. J.; Corn, R. M. *Anal. Chem.* **2004**, *76*, 6173–6178.
- (7) Lagally, E. T.; Emrich, C. A.; Mathies, R. A. *Lab Chip* **2001**, *1*, 102–107.
- (8) Liu, Y. J.; Rauch, C. B.; Stevens, R. L.; Lenigk, R.; Yang, J. N.; Rhine, D. B.; Grodzinski, P. *Anal. Chem.* **2002**, *74*, 3063–3070.
- (9) Bhattacharya, S.; Salamat, S.; Morisette, D.; Banada, P.; Akin, D.; Liu, Y. S.; Bhunia, A. K.; Ladisch, M.; Bashir, R. *Lab Chip* **2008**, *8*, 1130–1136.

- (10) Koh, C. G.; Tan, W.; Zhao, M. Q.; Ricco, A. J.; Fan, Z. H. *Anal. Chem.* **2003**, *75*, 4591–4598.
- (11) Matsubara, Y.; Kerman, K.; Kobayashi, M.; Yamamura, S.; Morita, Y.; Tamiya, E. *Biosens. Bioelectron.* **2005**, *20*, 1482–1490.
- (12) Pavlovic, E.; Lai, R. Y.; Wu, T. T.; Ferguson, B. S.; Sun, R.; Plaxco, K. W.; Soh, H. T. *Langmuir* **2008**, *24*, 1102–1107.
- (13) Umek, R. M.; Lin, S. W.; Vielmetter, J.; Terbrueggen, R. H.; Irvine, B.; Yu, C. J.; Kayyem, J. F.; Yowanto, H.; Blackburn, G. F.; Farkas, D. H.; Chen, Y. P. *J. Mol. Diagn.* **2001**, *3*, 74–84.
- (14) Liu, R. H.; Yang, J. N.; Lenigk, R.; Bonanno, J.; Grodzinski, P. *Anal. Chem.* **2004**, *76*, 1824–1831.
- (15) Yeung, S.-W.; Lee, T. M.-H.; Cai, H.; Hsing, I.-M. *Nucleic Acids Res.* **2006**, *34*, e118.
- (16) Yeung, S. S. W.; Lee, T. M. H.; Hsing, I. M. *Anal. Chem.* **2008**, *80*, 363–368.
- (17) Sanchez, J. A.; Pierce, K. E.; Rice, J. E.; Wangh, L. J. *Proc. Natl. Acad. Sci. U.S.A.* **2004**, *101*, 1933–1938.
- (18) Mix, M.; Reske, T.; Duwensee, H.; Flechsig, G.-U. *Electroanalysis* **2009**, *21*, 826–830.
- (19) Reske, T.; Mix, M.; Bahl, H.; Flechsig, G. U. *Talanta* **2007**, *74*, 393–397.
- (20) Luo, X. T.; Lee, T. M. H.; Hsing, I. M. *Anal. Chem.* **2008**, *80*, 7341–7346.

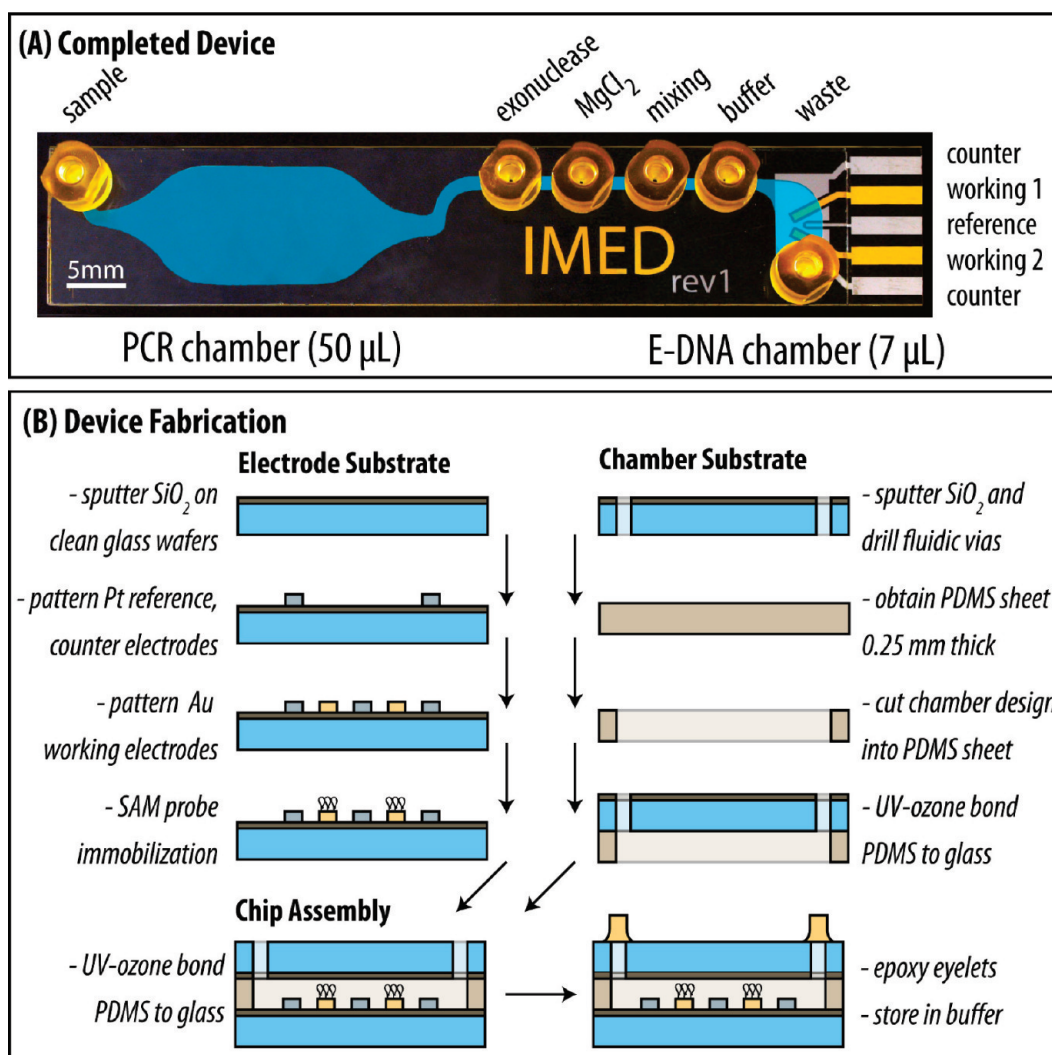


Figure 1. IMED device architecture and fabrication. (A) The completed chip measures 73 mm \times 13 mm and has six fluidic inlet/outlets (sample, lambda exonuclease, $MgCl_2$, mixing, E-DNA buffer, and waste). The PCR and E-DNA detection chambers have capacities of 50 and 7 μ L, respectively. The detection chamber incorporates two gold working electrodes (area = 1.5 mm²), a platinum counterelectrode (area = 19 mm²), and a platinum reference electrode (area = 0.42 mm²). (B) The device is composed of a PDMS layer between two silicon dioxide-passivated glass wafers. (Left) The electrodes are patterned on the bottom wafer by standard photolithography and are incubated with thiol-terminated E-DNA probes and a C6 passivation layer. (Right) Fluidic vias are drilled into the top glass wafer, and the PDMS chamber layer is bonded to it after UV-ozone treatment. (Bottom) The two substrates are aligned and bonded after UV-ozone treatment. Fluidic connectors are affixed with epoxy.

DNA (IMED) sensor (Figure 1A). First, the system performs symmetric PCR to rapidly amplify target DNA while incorporating phosphorylated primers into one strand of each duplex. We then introduce lambda exonuclease enzymes²¹ into the chip to selectively digest the phosphorylated strands and produce ssDNA products. Finally, the ssDNA is directed to an integrated reagentless, sequence-specific electrochemical DNA sensor (E-DNA)^{22,23} that detects target amplicons within the chip. As a model, we demonstrate detection of the *GyrB* gene of *Salmonella enterica* serovar Typhimurium LT2 from genomic DNA samples with a limit of detection (LOD) below 10 aM, roughly a 100-fold improvement over asymmetric PCR-based electrochemical methods.

EXPERIMENTAL METHODS

Chip Design and Fabrication. The fabrication process utilizes a modular architecture wherein the electrode substrate and the chamber substrate are fabricated separately, and assembled as a post-process (see Figure 1B). Both substrates are fabricated from 4-in.-diameter, 500- μ m-thick borofloat glass wafers (Precision Glass and Optics, Inc., Santa Ana, CA). To fabricate the electrode substrate (Figure 1B, left), the wafers are first passivated with a 100-nm-thick layer of sputtered SiO_2 . Then the counter and reference electrodes (20 nm Ti/250 nm Pt) are patterned via the lift-off process after standard photolithography. The working electrodes (20 nm Ti/250 nm Au) are then patterned using the same process. Next, the wafer is diced and cleaned with acetone, isopropanol, and deionized water (3 min each), followed by piranha solution (5 min). Subsequently, the E-DNA probes are allowed to self-assemble on the gold working electrodes via gold–thiol bonds. The chamber substrate

(21) Little, J. W. *Gene Amplif. Anal.* **1981**, *2*, 135–145.

(22) Fan, C. H.; Plaxco, K. W.; Heeger, A. J. *Proc. Natl. Acad. Sci. U.S.A.* **2003**, *100*, 9134–9137.

(23) Lai, R. Y.; Lagally, E. T.; Lee, S. H.; Soh, H. T.; Plaxco, K. W.; Heeger, A. J. *Proc. Natl. Acad. Sci. U.S.A.* **2006**, *103*, 4017–4021.

(Figure 1B, right) is fabricated by depositing a 100-nm-thick SiO₂ passivation layer and drilling fluidic vias (1.1 mm in diameter) with a CNC mill (Flashcut CNC, San Carlos, CA) equipped with a diamond bit (Triple Ripple, Abrasive Technology, Lewis Center, OH). The microfluidic channels are patterned out of a 250- μ m-thick polydimethylsiloxane (PDMS) sheet using a cutting plotter (CE5000-60, Graphtec, Santa Ana, CA). The PDMS layer is treated with UV-ozone (300 s) and permanently bonded to the chamber substrate. The two substrates are assembled using the same UV-ozone bonding applied to the PDMS layer (Figure 1B, bottom). Finally, the eyelets (Labsmith, Inc., Livermore, CA) are affixed to the vias with 5-min epoxy (Devcon, Danvers, MA), and the chip is filled with phosphate-buffered saline (PBS) until use.

DNA Sequences. The PCR primer and E-DNA probe sequences to detect the *GyrB* gene of *Salmonella enterica* serovar Typhimurium LT2 are adopted from our previous work.²³ The forward primer is 5'-GGA AAC CAT CGT TCC ACT-3', and the reverse primer is 5'-5Phos/AAC AAG AAT AAA ACG CCG AT-3' (Integrated DNA Technologies, Inc., Coralville, IA). We note that the 5' end of the reverse primer is phosphorylated, such that this strand will be selectively digested by the lambda exonuclease enzyme to yield ssDNA products of the following sequence: 5'-GGA AAC CAT CGT TCC ACT GCA GCG CTA CTT CCA CGC CGA TAC CGT CTT TTT CGG TGG AGA AAT AGA AGA TAT TCG GGT GGA TCG GCG TTT TAT TCT TGT T-3'. The E-DNA probe was synthesized by Biosearch Technologies (Novato, CA) with the following sequence: 5'-HS-(CH₂)₁₁-GCA GTA ACA AGA ATA AAA CGC CAC TGC-(CH₂)₇-NH₂-MB-3'. A 17-base complementary sequence (underlined) is used for the detection.

E-DNA Probe Preparation. The Methylene Blue redox-labeled E-DNA probe is immobilized on the gold electrodes via thiol bonding, and the electrode surface is passivated with 6-mercapto-1-hexanol (C6), as described in our previous work.^{12,23} Because E-DNA detection is performed without any purification steps, the sensor surface must be desensitized to protein-rich samples. This is achieved by incubation of the sensor with a 1 \times Hotstar master mix (Qiagen, Venlo, The Netherlands) without template or primers and 0.1% bovine serum albumin (BSA) for 30 min and then flushing with guanidine hydrochloride. This is repeated twice or until the baseline alternating current voltammetry (ACV) signal becomes stable.

PCR Protocol. Genomic DNA of *Salmonella* was obtained from ATCC (Manassas, VA) and reconstituted in TE buffer (10 mM Tris, 1 mM EDTA, pH 7.5) at 1 ng/ μ L. The PCR mix (100 μ L) consists of 50 μ L 2 \times Hotstar Taq master mix, 42 μ L RNase-free water, 300 nM forward primer (3 μ L), 300 nM phosphorylated reverse primer (3 μ L), 20 μ g BSA (1 μ L, Sigma Aldrich, St. Louis, MO), and 1 μ L *Salmonella* template DNA diluted from stock to obtain the desired concentration. The sample is then injected into the PCR chamber in the chip, and excess sample is eluted through the mixing port to prevent it from entering the E-DNA chamber. To perform thermal cycling, the PCR chamber of the IMED chip is placed next to a 100 Ω platinum resistive temperature detector (RTD) mounted onto a custom thermofoil heating pad (Minco, Minneapolis, MN), which is driven by a temperature controller (Omega Engineering, Inc., Stamford, CT). The chip is subjected to a 15-min, 94 $^{\circ}$ C hot start, 38 cycles of PCR at 94 $^{\circ}$ C, 55, and 72

$^{\circ}$ C (with ramps of \sim 15, \sim 30, and \sim 10 s, respectively, and 30 s dwells) and 5 min final extension at 72 $^{\circ}$ C over \sim 90 min. During thermocycling, the E-DNA chamber is kept at 18 $^{\circ}$ C with a thermoelectric cooler (Laird Technologies, Chesterfield, MO).

On-Chip Single-Stranded DNA Generation. The lambda exonuclease enzyme was purchased from New England Biolabs (Ipswich, MA). The PCR product and stock enzyme are pumped simultaneously at a flow-rate ratio of 10:1 (200 and 20 μ L/min for product and enzyme respectively), meeting in the channel and exiting the chip through tubing at the mixing port into an empty microcentrifuge tube. The mixture is then drawn back into the PCR chamber, and incubated for 20 min at 37 $^{\circ}$ C via our temperature controller. The effectiveness of the mixing scheme was tested empirically; buffer and blue dye (to simulate the enzyme) were used in the same manner. The fluids appeared uniformly mixed upon entry into the microcentrifuge tube (data not shown).

AC Voltammetry. The electrodes are connected to an electrochemical analyzer (CH Instruments, Inc., Austin, TX) via a standard five-pin card-edge connector. ACV is performed between -0.75 V and -0.25 V at a frequency of 10 Hz and sensitivity of 200 nA/V. To verify all signals, ACV scans were performed in triplicate. To accommodate the on-chip platinum pseudo-reference electrodes, curve alignment was performed based on the peak current.¹²

On-Chip E-DNA Measurements. Samples are introduced to the E-DNA chamber with a syringe pump (Harvard Apparatus, Holliston, MA). All ACV scans are conducted when the chamber is filled with PBSM buffer (1 \times PBS increased to 50 mM MgCl₂), which matches the salt concentration of the sample. To establish the baseline, 1 mL of PBSM is pumped through the chamber and ACV scans are obtained. Next, the sample is mixed with MgCl₂ (in the same manner as lambda exonuclease), boosting the salt concentration to 50 mM to expedite hybridization of the target to the sensor. The sample is then pumped into the E-DNA chamber, where it incubates with the sensor for 20 min, and the ACV signal is obtained. Finally, the E-DNA probe is regenerated by pumping 1 mL of 8 M guanidine hydrochloride followed by 5 mL of deionized water through the chamber.

Negative Controls. IMED chips were designed to be disposable for one-time use, akin to a PCR tube, to avoid carry-over contamination. As such, negative controls could not be run on the same chip. Instead, for each IMED trial, a corresponding zero-template negative control was simultaneously conducted in a benchtop thermal cycler (Eppendorf, Westbury, NY) under the same protocol. Each was then used to challenge the regenerated E-DNA sensor after the corresponding IMED trial (see purple curves in Figure 5, presented later in this work). Furthermore, to verify that the chip is not a source of contamination, a zero-template negative control IMED trial was also performed (see Figure 5A, presented later in this work).

RESULTS AND DISCUSSION

IMED Chip Design. The IMED system integrates three main biochemical functions, which are performed sequentially on a single monolithic chip: (1) exponential PCR amplification, (2) enzymatic conversion from double-stranded (ds) PCR amplicons

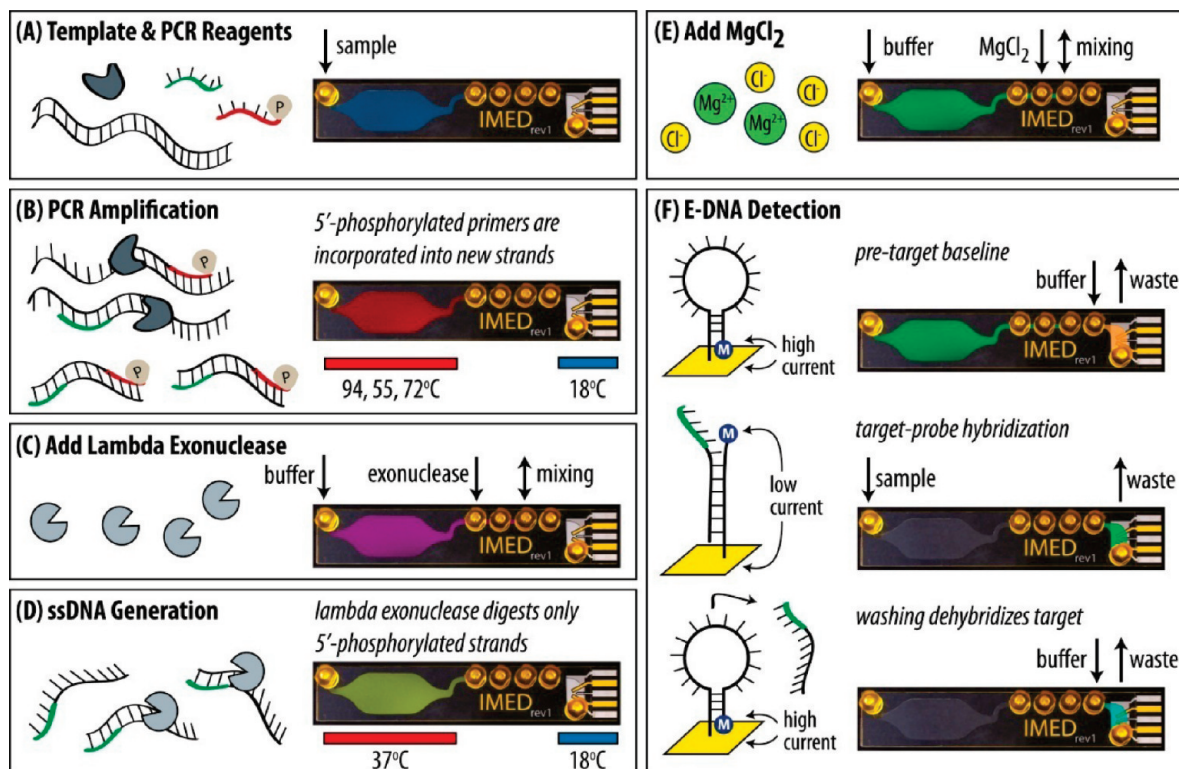


Figure 2. IMED assay overview. (A) Template DNA is added to a PCR reagent mixture containing phosphorylated reverse primers. (B) The template is PCR amplified. (C and D) Lambda exonuclease is mixed with the product and digests the phosphorylated strands. (E) Prior to electrochemical analysis in the detection chamber, $MgCl_2$ is added to the IMED chip to adjust the salt concentration from 1.5 mM to 50 mM to optimize the hybridization conditions. (F) Before introducing sample to the sensor, a baseline redox current is measured via ACV. Next, the ssDNA product hybridizes with the E-DNA probe modulating the redox current signal. Finally, the E-DNA probe is regenerated to verify the hybridization event.

into target ssDNA, and (3) sequence-specific electrochemical detection. First, genomic DNA and PCR reagents are loaded into the PCR chamber (see Figure 2A) and thermal cycling is performed using a temperature-controlled thermofoil (see Figure 2B). During PCR, the reverse primers yield phosphorylated strands, which are subsequently selectively digested by lambda exonuclease within the PCR chamber to efficiently produce ssDNA targets for detection (see Figures 2C and 2D). Next, the salt concentration is modified for optimal hybridization (see Figure 2E), and sequence-specific electrochemical detection is performed with E-DNA probes,^{12,22–24} where target hybridization causes a change in the redox current of the probe, which is detected via ACV (see Figure 2F).

Integrated PCR and Single-Strand Generation. We achieved highly efficient exponential PCR amplification and enzymatic generation of ssDNA in the IMED chip (see Figure 3). To prevent polymerase adsorption to the walls during the reaction, glass surfaces were coated with 100 nm of SiO_2 , and 0.1% BSA was added in solution to act as a dynamic coating.²⁵ The sample loading rate was optimized at 200 $\mu L/min$ to prevent bubble formation. The IMED chip yielded double-stranded PCR amplicons of the correct size (100 bp) after 38 cycles (see Figure 3, lane 4), and the efficiency was comparable to that of a

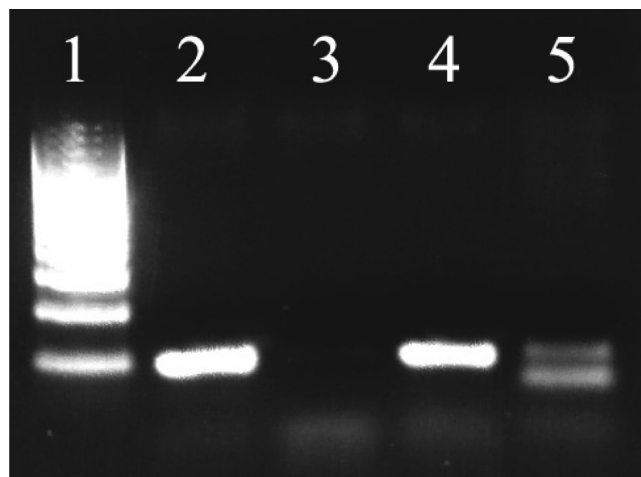


Figure 3. Demonstration of on-chip PCR and ssDNA generation. Lane 1, 100 base-pair ladder; lane 2, positive control from benchtop thermal cycler; lane 3, negative control from the IMED chip without template DNA; lane 4, IMED output with template DNA, which showed similar efficiency to the benchtop thermal cycler; and lane 5, IMED output after ssDNA generation. The lower band is ssDNA and upper band indicates incompletely digested double-stranded DNA.

benchtop thermocycler (lane 2 in Figure 3). As expected, the IMED chip did not produce target amplicons without template DNA (lane 3).

ssDNA was generated by incubating the dsDNA amplicons with the lambda exonuclease for 20 min in the chip. The phosphorylated strands of the dsDNA were efficiently digested,

(24) Lubin, A. A.; Lai, R. Y.; Baker, B. R.; Heeger, A. J.; Plaxco, K. W. *Anal. Chem.* **2006**, *78*, 5671–5677.

(25) Zhang, C. S.; Xing, D. *Nucleic Acids Res.* **2007**, *35*, 4223–4237.

E-DNA Sensor Response

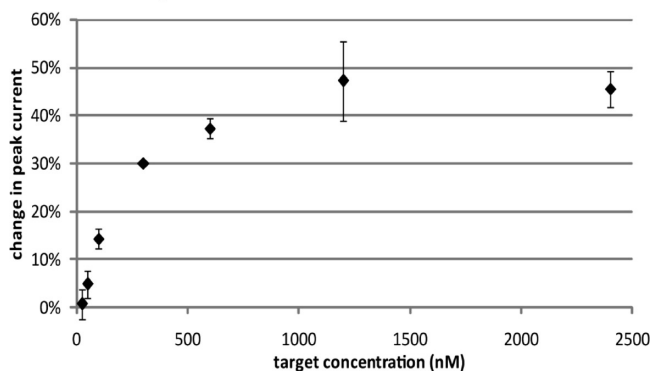


Figure 4. E-DNA sensor response as a function of concentration. The E-DNA sensor signal, as represented by the percent change in peak current between the baseline and after incubation with synthetic DNA target for 30 min. The standard deviation for each point was calculated from three measurements from three separate chips.

yielding ssDNA targets ready for E-DNA detection (see Figure 3, lane 5). The lower band in this lane corresponds to the ssDNA, which has higher electrophoretic mobility, whereas the upper band is representative of undigested dsDNA amplicons. Importantly, we note that the fluorescent stain (Lonza GelStar* Nucleic Acid Gel Stain, Thermo Fisher Scientific, Waltham, MA) is significantly more efficient in labeling dsDNA, compared to ssDNA; although we observed a clearly visible dsDNA band in the gel, measurements of fluorescence relative to a controlled mass standard indicated that the yield of this enzymatic reaction was >90% (data not shown).

On-Chip E-DNA Detection. The dose–response calibration curve of the on-chip E-DNA sensor module was characterized over a wide range of concentrations (25–2400 nM) using a protocol developed from earlier work^{22,23,26} (see Figure 4). To measure chip-to-chip variability, three different chips were tested at each concentration. The resulting standard deviation from all measurements was ~3%, indicating that our chip fabrication and sensor preparation steps are highly reproducible. We note that successive scans using the same electrode yielded an average standard deviation in peak current of ~1.5%, which is inherent to the probe chemistry.²⁷ We attribute additional variations of the peak current between chips to alignment errors during the chip assembly, which result in variations in the effective electrode surface area.

Integrated System Performance. We performed a complete IMED assay for the detection of the *Salmonella GyrB* target, and the resulting AC voltammograms are shown in Figure 5. First, baseline ACV curves were obtained for each chip (blue curves in Figure 5); as expected, the sensor yields a negligible change in peak faradaic current (<1%, compared to the average background noise of 1.5%) when challenged with a sample that contained no template DNA (see red curve in Figure 5A). On the other hand, the sample that contained 100 aM *Salmonella* genomic DNA induced a 52% decrease in the peak current (see red curve in Figure 5B). Furthermore, we verified that this reduction in current is indeed caused by hybridization between target ssDNA and

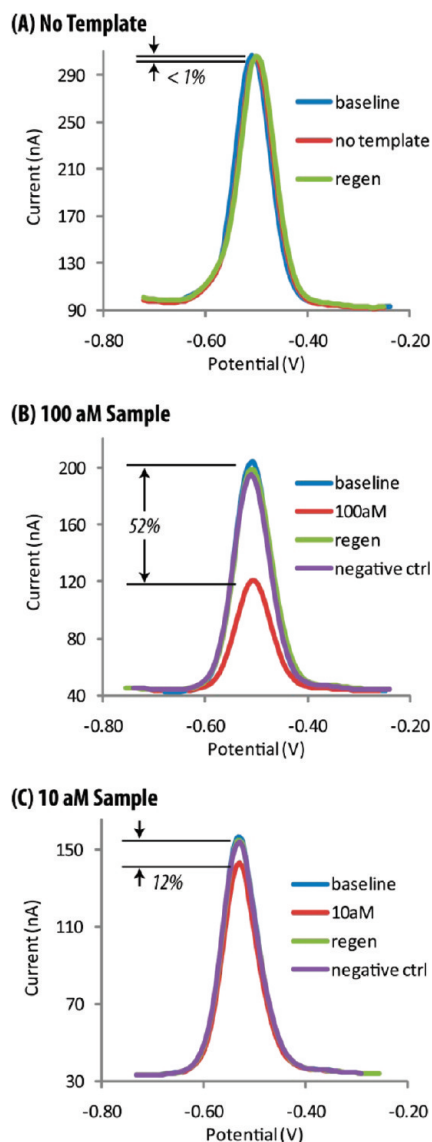


Figure 5. Limits of IMED detection with *Salmonella* genomic DNA. (A) The no-template negative control yielded <1% change in the faradaic current (red) compared to the baseline (blue). Probe regeneration with guanidine hydrochloride reset the sensor to within 98% of its initial state (green). (B) The 100 aM sample produced a 52% signal change, and (C) the 10 aM sample produced a 12% signal change, with respect to the baseline (red, blue). Each detection was validated with sensor regeneration, which returned the probe current to >96% of the baseline (green). Signals in panels B and C were also compared against externally prepared zero-template negative controls, which resulted in drops of 1% and 0%, respectively (purple).

E-DNA probes by regenerating the sensor, which returns the current signal to within 96% of the initial baseline (see green curve in Figure 5B). The sample that contained 10 aM template DNA produced a 12% decrease in peak faradaic current, with the signal returning to 98% of the initial baseline after regeneration (see red and green curves in Figure 5C). To further verify the signal, the sensors were challenged with external zero-template negative controls prepared in a benchtop thermocycler (Eppendorf, Westbury, NY), producing little change from the regenerated signal levels, with signal drops of 1% (100 aM sample) and 0% (10 aM sample) (see purple curves in Figures 5B and 5C).

(26) Ricci, F.; Lai, R. Y.; Heeger, A. J.; Plaxco, K. W.; Sumner, J. J. *Langmuir* **2007**, *23*, 6827–6834.

(27) Murphy, J.; Cheng, A.; Yu, H.-Z.; Bizzotto, D. J. *Am. Chem. Soc.* **2009**, *131*, 4042–4050.

We have demonstrated the aforementioned results, based on the concentration of purified *E. coli* genomic DNA. To estimate the device performance, in terms of colony-forming units (CFU), we have used a simple calculation based on the work of Churchward et al.²⁸ Assuming a doubling time of 40 min²⁹ and complete cell viability in a similar 50- μ L sample, we estimate that our 10 aM and 100 aM signals would correspond to \sim 120 and \sim 1200 CFU, respectively.

CONCLUSION

The Integrated Microfluidic Electrochemical DNA (IMED) system represents a completely integrated electrochemical DNA detection architecture with a limit of detection of <10 aM (\sim 300 copies in our chamber size), which is \sim 2 orders of magnitude below that of previously reported work.^{13–16} While previous methods based on asymmetric PCR exhibited limited efficiency, IMED exponentially increases the target concentration through symmetric polymerase chain reaction (PCR). This is enabled by lambda exonuclease, which converts dsDNA into ssDNA within minutes. Incorporation of enzymatic digestion into the IMED workflow was facile to implement, because the enzyme operates effectively in unmodified PCR buffer.

The disposable microfluidic architecture minimizes sample loss and the likelihood of contamination because the fluid pathways are contained within a sterile system. One particularly noteworthy feature of the device fabrication process is the use of an electronic cutting plotter to define the channel patterns in the PDMS sheet;

- (28) Churchward, G.; Bremer, H.; Young, R. J. *Theor. Biol.* **1982**, *94*, 651–670.
(29) Gordon, D. M.; Riley, M. A. *Mol. Microbiol.* **1992**, *6*, 555–562.

this immediate CAD-to-prototype method allows convenient and rapid fabrication. The device can also be used for the detection of RNA, as well as DNA, through the use of reverse transcriptase enzymes. In addition, through the use of different redox labels or electrode-specific probe immobilization, IMED can be expanded to enable multiplex detection.¹² We believe that the inherent limit of detection can be brought significantly lower than 10 aM through optimization of the PCR protocol. For example, after performing the PCR/exonuclease reaction with a 100 zM sample (roughly three copies for our chamber size) in a benchtop instrument, we observed a 9% change in signal, compared to a change of $<1\%$ in the negative control (see Figure S1 in the Supporting Information). Considering that a variety of methods already exist for extracting nucleic acids from raw samples,^{30–32} we believe that the IMED system represents an important step toward genetic detection at the point of care.

SUPPORTING INFORMATION AVAILABLE

Figure S1 shows the E-DNA sensor response against optimized PCR product. (PDF) This material is available free of charge via the Internet at <http://pubs.acs.org>.

Received for review April 30, 2009. Accepted June 19, 2009.

AC900923E

- (30) Huang, Y.; Mather, E. L.; Bell, J. L.; Madou, M. *Anal. Bioanal. Chem.* **2002**, *372*, 49–65.
(31) Purdy, K. J. In *Environmental Microbiology*; Elsevier Academic Press: San Diego, CA, 2005; Vol. 397, pp 271–292.
(32) Berensmeier, S. *Appl. Microbiol. Biotechnol.* **2006**, *73*, 495–504.